GEOLOGICA BELGICA (2014) 17/1: 52-57

Network approach to assess the impact of ghost-rock karsts located in the neighbourhood of masonry structures

Laurent VAN PARYS[1], Jérôme NOEL[1], John DECEUSTER[2] & Georges KOUROUSSIS[3]

[1]*UMONS – Dept of Civil Engineering, Place du Parc 20, 7000 MONS*
[2]*UMONS – Dept of Geology and Applied Geology, Place du Parc 20, 7000 MONS*
[3]*UMONS - Dept of Theoretical mechanics, Dynamics and Vibrations, Place du Parc 20, 7000 MONS*

ABSTRACT. Efficient for erecting buildings based on small-size elements, unreinforced masonry is used since centuries in many places around the world. The intrinsic mechanical weaknesses that they exhibit can however reveal problematic when subject to parasite actions. Asleep under buildings, ghost-rock karst constitutes therefore a severe threat: any external action is likely to activate it; leading to potential modification of the ground bearing capacities and then eventually inducing irreversible damages to the masonry. When building in such critical zones, architects have to integrate karst risks from the very beginning of their mission by relying on building specialists who focus their attention on the limitation of the concerned structures vulnerability. To achieve their aim, these engineers have to estimate to which extent a ground defect, induced by an activated ghost-rock karst and appearing in the neighbourhood of a given masonry building, is likely to damage it. In continuity with stability studies, these structural experts involved in karst risk management commonly establish a great number of scenarios and analyse them by simulating the soil-structure interaction problems using commercial finite element codes. To overcome interpretation difficulties, post-processing facilities can reveal of great interest for the exploitation of numerical results. We present here a network approach to automate the post-processing of soil-structure interactions and help assessing the impact of ghost-rock karsts on masonry structures. Following a transdisciplinary presentation of the problematic, we detail the approach for automatically quantifying the impact of a karst-induced soil defect. We then describe a practical implementation and illustrate the feasibility of the proposed methodology on a case study.

KEYWORDS: ghost-rock karsts, masonry, pathology, numerical simulation, post-processing

1. Densification of built tissues, karstic context and severe threat for buildings

Although timescales associated with geological and architectural questions are rarely comparable, particular contexts can impose gathering both aspects. Once the world demographic growth is considered in relationship with land planning programs that dedicate more and more zones to non-building purposes, a limitation in land offer appears concomitantly with an expansion of land demand. Then, contemporary architects have to localize more and more building projects in zones that remain available for erecting usages, whatever are the suitability of ground capabilities or the compatibility with the surrounding environment. Around the world, many critical zones dedicated to erecting usages are affected by the presence of karst features. When occurring in urbanized areas, associated sinkhole collapses can cause considerable damage on buildings and infrastructures, sometimes leading to their complete destruction and losses of human lives. Well-known cases have been reported all around the world and representative examples of severe damages can be found in: Sowers, 1996 (Winter Park, Florida, USA), Buttrick & van Schalkwyk, 1998 (Gauteng Province in South Africa), Yuan et al., 1998 (southern China), Dougherty, 2005 (Allentown Corporate Plaza in Pennsylvania, USA), Buchignani et al., 2008 (Camaiore city in Tuscany, Italy) and Kaufmann et al., 2012 (Rieu de Warchin site in Tournaisis, Belgium). Unlike geological specialists who mainly consider bedrock alterations through the prism of rock weathering evolving in conjunction with tectonic phenomena, the builders follow a pragmatic outlook: the ground is the support on which buildings are settled and bedrock alterations can potentially cause serious structural problems. To limit the vulnerability of the considered buildings, the architects mandate structural experts who have to discriminate between two geological aspects integrated to their practice: asleep and awake ghost-rock karsts.

In the Tournaisis (see section 4 below), the bedrock is mainly composed of argillaceous and siliceous Carboniferous limestone. This bedrock is overlain, in a non-uniform way, by a cover that mainly consists of Cretaceous marls and chalks and sandy or clayey Tertiary sediments. The thickness of this cover ranges from a few meters near Tournai to more than 100 meters in the NW. Even if the fairly flat relief of the Tournaisis area shows few landforms typical of karst terrains, quarry faces suggest that palaeokarst features are common in the underlying limestone (e.g., Vergari et al., 1995, Kaufmann & Quinif, 1999, Kaufmann, 2000). These features formed prior to the deposit of the Tertiary sediments and mostly develop associated to discontinuity planes (joints) by progressive dissolution of the carbonates leaving a soft and porous weathering residue called ghost-rock (e.g., Quinif, 2010, Dubois et al., 2014). A typical result of this weathering process is a profile with 1 to 10 meters wide and 10 to 30 m high slots (Sowers, 1996) between blocks of intact rock. The main specificity of this profile is that these slots mainly contain an isalterite (weathering product with slight or no change in rock volume and remnant rock structure), as defined by Delvigne (1998), except at their top. In most cases, this system is characterized by an equilibrium state and the building specialists refer to this situation as ‘asleep ghost-rock karst’. In the Tournaisis, most new sinkholes develop directly above these palaeokarst features (Kaufmann, 2000), mainly in areas of water table decline in the karst aquifer as shown by Kaufmann & Quinif (1999, 2002). As a consequence of dewatering, the equilibrium state is broken. Underground voids develop by isalterite compaction and/or collapse and transport phenomena will induce the evacuation of residual materials (Quinif, 2010). Such an evacuation induces the formation of underground cavities and the building specialists refer to this situation as ‘awake ghost-rock karst’. Besides the occurrence of impressive sinkhole collapses, such cavities migrating upwards through soil layers can locally modify the bearing capabilities of the ground and then potentially impact the stability of sensitive built systems.

Formerly, buildings could be erected in unawareness of the karstic threat as the presence of karstic features could remain unknown until sinkhole collapses reach the surface. Since more than ten years, a set of ‘karstic constraints maps’ derived from hazard susceptibility maps, is available for land-use planning at a regional scale in the Walloon Region of Belgium (Van Dijck & Michel, 2006). This set shows sizeable areas of medium or high karstic constraint where the knowledge of local underground conditions has to be improved before erection is allowed, requiring geotechnical and/or geophysical investigations (e.g., Kaufman & Quinif, 2002, Deceuster et al., 2006, Kaufmann et al., 2012, Kaufmann & Deceuster, 2014) to detect and delineate palaeokarst features. Thanks to these maps, the architects can know if their buildings are located in critical zones (presence of asleep ghost-rock karsts). Depending on the mechanical properties of the cover materials, the size and shape of the cavity expected at the surface can be estimated by geological specialists (Kaufmann,

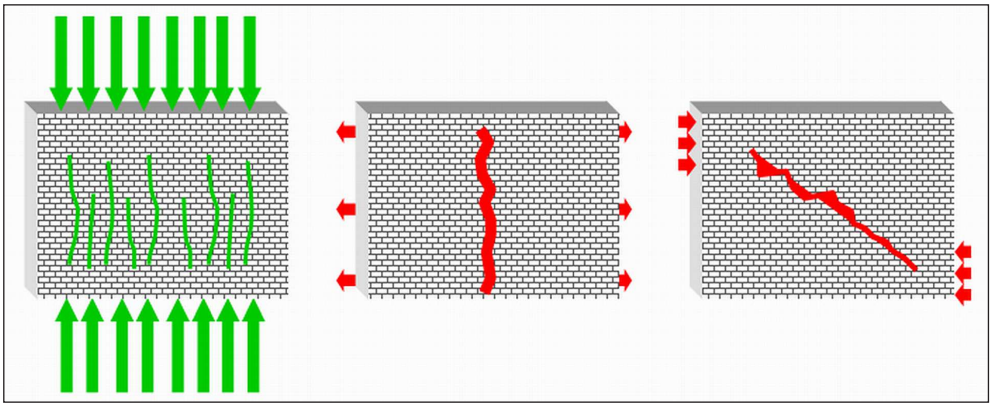

Figure 1. URM - capabilities in compression and limitations in tension or shear

2000). Although larger shapes have been reported, subsidence sinkholes in the Tournaisis are usually circular or elliptical in plan and cylindrical or conical in profile while diameter and depth commonly range between 5 and 10 m (Kaufmann & Quinif, 1999). Such information reveals fundamental in the practice of structural experts involved in vulnerability studies.

2. Weaknesses in masonry, vulnerability question and soil-structure simulations

Unreinforced masonry (URM) is a building material that is obtained by assembling small-size elements (clay bricks or stone blocks) with a mortar. With regard to this mode of erection, comfortable capabilities they exhibit towards compressive actions should always be nuanced by limitations concerning the response to tensile or shear loadings (Fig. 1). Despite such intrinsic weaknesses, masonry buildings are widespread all around the world. Nevertheless, as soon as a parasite phenomenon (e.g. local modifications of bearing capacity in the ground, vibrations transferred through the ground) mobilizes a weakness, pathologies are likely to appear in the structure. Depending on the relative capacities of mortars and masonry elements, the consequences can range from deformations to crack propagations (Fig. 2) which can ultimately lead to building collapses.

In critical zones (presence of asleep ghost-rocks), it is impossible to ensure that karst features will not become activated and underground cavities will not appear at the architect timescale (~100 years). Building specialists have thus to manage the associated risks by limiting the vulnerability of the masonry buildings towards the karst threat.

Despite the fact that several research teams investigate related topics, the evolution of an underground cavity (growth, upward migration…) based on soil data and possible water flow remains hardly predictable. The structural experts mandated by architects overcome this difficulty by considering a wide range of problematic scenarios likely to affect the studied structure. The pertinent *establishment of scenarios* is not a problem for engineers who are used to rely on the combination of different actions (wind, snow, fire…) in their stability studies. They consider complementarily to these commonly considered actions the possible shapes, sizes, positions and depths of an underground cavity. For every problematic scenario, they check the safety of the building or prescribe a local reinforcement solution. Therefore, every case studied by the architect is a prototype characterized by a specific morphology for the building, specific properties for the masonry, specific actions on the structure and specific characteristics for the karst threat (shape, size and location of the cavities). Building specialists are used to rely on commercial CAD tools based on the finite element (FE) method to study structural problems presenting complicated morphologies and/or load patterns. For every scenario, they opt for coupled soil-structure models enabling potential force redistributions inside the masonry based on the evolution of rigidities inside the system (Van Parys et al., 2006). Appreciating the vulnerability in each scenario by relying on FE results is the crucial point. In fact, coupled calculations provide rich results under the shape of general stress field maps. To estimate the extent to which the considered masonry structure would suffer from an awaked ghost-rock, building specialists have to compare the stress field maps associated to a reference case (without ground defect) to the ones associated to the problematic scenarios considered (with ground defect). They have then to express conclusions in terms of damages on structures. When considering several scenarios, a manual approach definitely reveals as highly time consuming. The *challenge thus consists in partially automating the interpretation process.* A possible approach consists in using a macro-element calculation scheme. This could bring interesting results but we did not privilege this solution due to practical reasons (inter-operability). We propose a post-processing approach designed as plug-in routines compatible with FE codes commonly used in engineering offices. In a first time, building specialists perform FE calculations classically for the reference case and the problematic scenarios considered. In a second time, the stand alone interpretation tool is launched. The end-user can choose the structural member to be treated (e.g. a given wall inside the studied building), define a profile network he judges pertinent and indicate the path to previously obtained FE results files. The automated post-processing tool will then provide conventional graphs as the final interpretation and, ultimately, outline, for every problematic scenario, a value denoting the impact of the ground disturbance on the considered structural member (Fig. 3).

Figure 2. URM - pathologies induced by modification of local bearing capacity in the ground.

3. Post-processing with distributed network

3.1. Four-step articulated interpretation

We propose a four-step methodology to automatically estimate the impact of activated ghost-rock on URM structures. For the considered structural member inside the studied building, the first practical goal consists in **summarizing [S] the general stress field**. The use of a network of profiles specifically distributed on the structure allows focusing on information judged crucial by the engineer involved in the vulnerability study by picking up, from FE results, the minimal data to be stored for further manipulations. The second step is run in parallel and consists in **efficiently organizing [O] the summarized information** using a graphically-based system. A stress or strain state associated with either disturbed (service state with ground defect) or reference case (service state without ground defect) is expressed as a coded

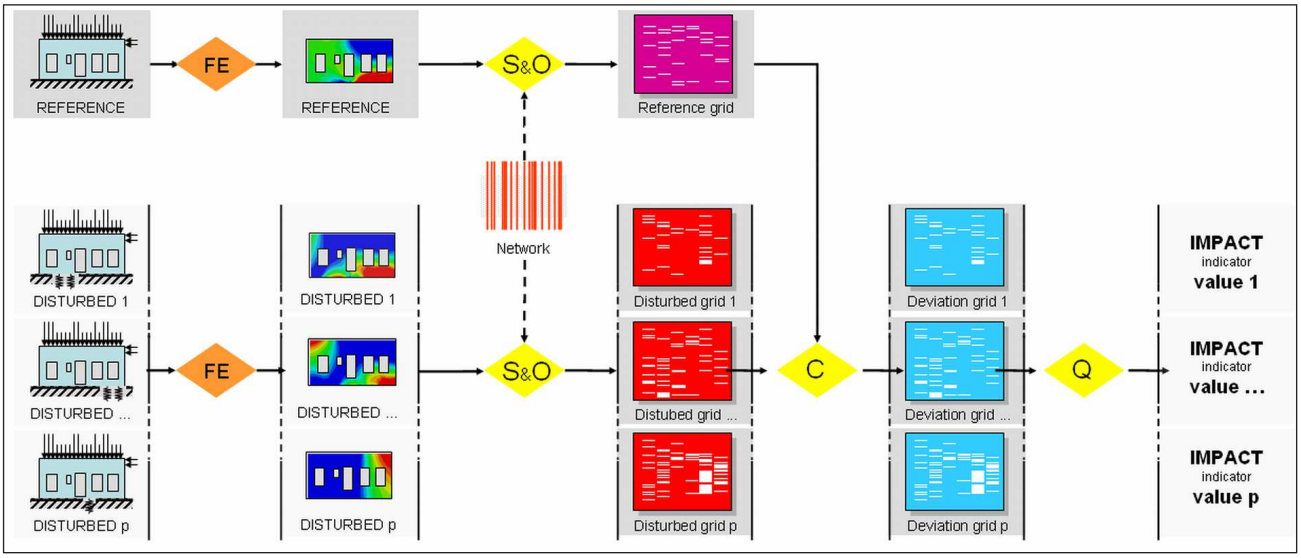

Figure 3. Appreciation of vulnerability towards the karstic threat based on FE computation.

grid. This graphically-based representation allows **performing comparisons [C]** in the third step by using pair-based approaches. It also further opens the way to image processing. In any case, the deviation between a disturbed and the reference case is expressed through an 'offspring' grid exhibiting the same typology as the 'parent' grids, visually documenting the impact of the disturbance. In the fourth step, a data integration scheme is implemented to conventionally **quantify [Q] the impact of this disturbance** using a single number indicator.

3.2 Summarizing data [S]: focused interest through distributed network

Numerical simulations provide rich results in terms of stresses or strains for each integration point. FE models enabling soil-structure interactions usually combine a large spatial extent to a suitable nodal discretization. Therefore, the size of stored result's matrices may become huge although a large part of them would reveal less useful in the interpretation. To focus on the crucial data, we propose to rely on the so-called network approach, inspired from researches (e.g., Maunder, 1995) that filled the gap between the intuitiveness of analytical approaches and the computational capacities offered by numerical simulations. A distributed network may be seen as an arbitrary collection of profiles that will be superimposed by the engineer on the considered structural member. As only the results collected along this grid of profiles will be extracted and considered in the next steps of the post-processing analysis, the network establishment process is of major importance to gain benefits in terms of efficiency. With specific skills and/or training concerning the behaviour of masonry structures, engineers are able to estimate the location of potentially critical zones in the structure. They can thus set a higher density of profiles in those areas while imposing a looser profile density elsewhere. The network varies for each case study but a single grid configuration is needed to perform every analysis inside a single interpretation batch (reference case and considered problematic scenarios).

3.3 Organizing summarized data [O]: technically-based formulation for results coding

After focusing on interesting data and reducing the storage needs, we implemented a reality-based filter to organize the data. This filter is based on technical aspects which would allow advantageously expressing meaningful considerations. A specific search engine associates a code to each stress or strain value that is encountered along profiles. It may for instance concern a potential steel requirement computed either through empirical rules or according to normative sources. The graphical representation of the coded results as a coded grid improves the understanding of the behaviour of the structure and allows the comparisons of several scenarios.

3.4 Comparing coded grids [C]: disturbance impact through deviation grid

Disturbed grids are compared to the reference grid to construct as many deviation grids as tested scenarios. The 'offspring' grids (deviation grids) and 'parent' grids are organized in the same manner. For models with a limited number of network profiles, the deviation grids are easily obtained through direct member-to-member matrix subtractions. For wider models, image processing techniques that allow the management of rich graphical datasets will be investigated to benefit from the graphical representation of the coded results. In any case, a deviation grid graphically expresses the impact of a given ground disturbance on the studied structural member given the profile network initially set up by the engineer. Its graphical character offers a global view of the disturbance impact on the structural member.

3.5 Quantifying the impact [Q]: integration scheme for indicator

Considering a reference, disturbed or deviation grid may already reveal useful as they present condensed information instead of general stress field maps. However, summarizing all the information contained in a grid by a single indicator value could be an efficient tool to automatically point out critical scenarios. A double level integration scheme like the one presented later (see 4) allows achieving this aim.

4. Implementation for illustrative purpose

To highlight the practical feasibility of the described methodology, this paragraph proposes a simple implementation of the post-processing tool and applies it to an illustrative case study taking place in the Tournaisis. The tool has been implemented inside the MATLAB environment and is used in conjunction with the commercial FE solver of SIMULIA.

4.1 Simplified tool and post-processing articulation

For the end-user, the overall process is articulated as follow.

1- The model of the masonry structure, its loadings and its environment are established in SIMULIA. A calculation is then carried out for the reference case and the *p* problematic scenarios, the mesh pattern of the masonry structure remains unchanged. Depending on the number of scenarios *p*, this process may be conducted either manually or automatically through a parametric approach piloted by a dedicated commercial tool.

2- Once the *p+1* FE result files (disturbed cases + reference case) are available, the MATLAB post-processing tool is launched. It will first ask the end-user to define a network for the further analysis. From the selection of nodes at the top edge of the mesh, the tool establishes the related distribution of vertical profiles.

3- Once the network is designed, the analysis is initiated

considering the FE result files as input data. The summarizing **[S]** module scans the files and exclusively extracts data associated to the highlighted profiles.

4- Once the restricted data has been collected, the organizing [O] module focuses, in the simplified scheme that has been implemented for illustrative purpose, on the local value of σ-stress considered acting orthogonally to the profile. Following a rough 'no tensile strength' assumption leads to compute a value of Local Steel Indicator LSIij = Aij.ξ(σ).σij for the level j (j = 1 … m_i) in profile i (i = 1… n) $LSI_{ij} = A_{ij}.x(s).s_{ij}$ where σ_{ij} is the local value of σ-stress obtained from the FE results, A_{ij} denotes the influence of area associated with σ_{ij} and ξ(σ) is a state variable whose value is 0 if $\sigma_{ij} \leq 0$ (local compression state) or $f_{steel,tension}^{-1}$ if $\sigma_{ij} > 0$ (local tension state). The computed values of LSI_{ij} for the *p+1* configurations are then used for establishing the disturbed and reference grids. Such a definition of the indicator denotes a fictitious section of steel that could balance any encountered tensile stress and opens the way to advanced coding.

5- Once the 'parent' grids are available, the comparison **[C]** module may establish deviation grids expressing, in the simplified scheme that has been implemented, the steel pattern that should be added to the reference case for complying with the considered disturbed scenario.

6- Based on the deviation grids, the quantification **[Q]** module performs, in this simplified case, an integration along the profile *i,* expressing a Profile Steel Indicator as $PSI_j = \Sigma_i LSI_{i,j}$ and, later, a Network Steel Indicator as $NSI=\Sigma_j PSI_j$. These *p* values of NSI are the global indicators that quantify the impact of the ghost-rock defect on the considered masonry structure for the *p* problematic scenarios.

4.2 Illustrative case study

This post-processing scheme is applied for carrying out an illustrative vulnerability study on the Choiseul seminary, a heritage masonry building erected several centuries ago in Tournai (BE). With around 48 m length, 12 m wide and 21 m high, the building presents its main entrance on the south elevation. One level is located downstairs, opening to the northern garden; three full levels are located upstairs as well as storage places inside the roof. Although the building has been erected in the Tournaisis, it has not been affected yet by karst-induced pathologies. The building specialists may thus consider the current situation as the **reference case**: the sandy-clayey soils provide a convenient load bearing capacity. A complete vulnerability study should concern each structural member of the building. For illustrative purposes we focused on the north elevation wall, the most

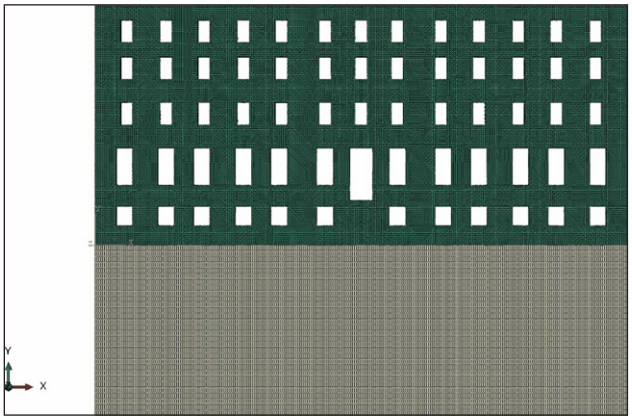

Figure 4. FE model presenting the wall and the ground for the reference case.

critical structural member due to the land declivity. Based on the knowledge of geological specialists, a wide range of problematic scenarios where cavities vary in shapes, sizes and locations could be considered as **disturbed cases**. The studied situations are modelled with structured three-dimensional discretization in SIMULIA (Fig. 4), presenting FE model of the considered wall interacting in conjunction with the ground. With almost 0.5 m thick, the north elevation wall supports a 1062 daN/m roof loading as well as 1200 daN/m floor loadings at each level. The wall is established with unreinforced plain masonry composed of clay bricks and limestone blocks assembled with a lime mortar. An equivalent material (Domede et al., 2009) has been proposed to simulate this complex structure. This material exhibits a simple elastic behaviour whose properties have been derived from lab tests conducted on similar materials collected for previous studies (Van Parys et al., 2006): density = 1.8, elastic modulus = 20000 MPa, Poisson's ratio = 0.2. The effects of bearing walls and steel ties established orthogonally to the studied wall are replicated by constraining degrees of freedom in the concerned directions (Descamps et al., 2011). Although more complicated approaches are available (Kouroussis et al., 2011), a simple approach (Van Parys et al., 2006) is used to simulate the ground located around the building (an elastic model with continuity conditions acting orthogonally to the modelled plane: density = 1.8, elastic modulus = 1000 MPa, Poisson's ratio = 0.3). In addition to the reference case, three potentially problematic scenarios presenting an elliptic

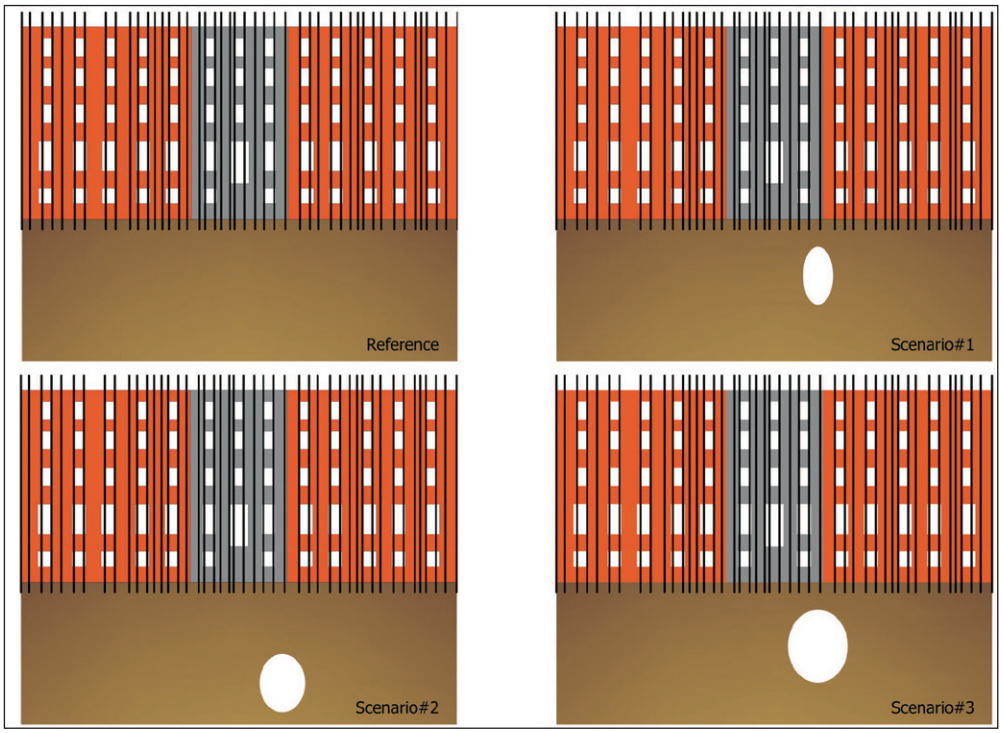

Figure 5. North elevation wall: one reference case & three highlighted scenarios with the analysis network superimposed.

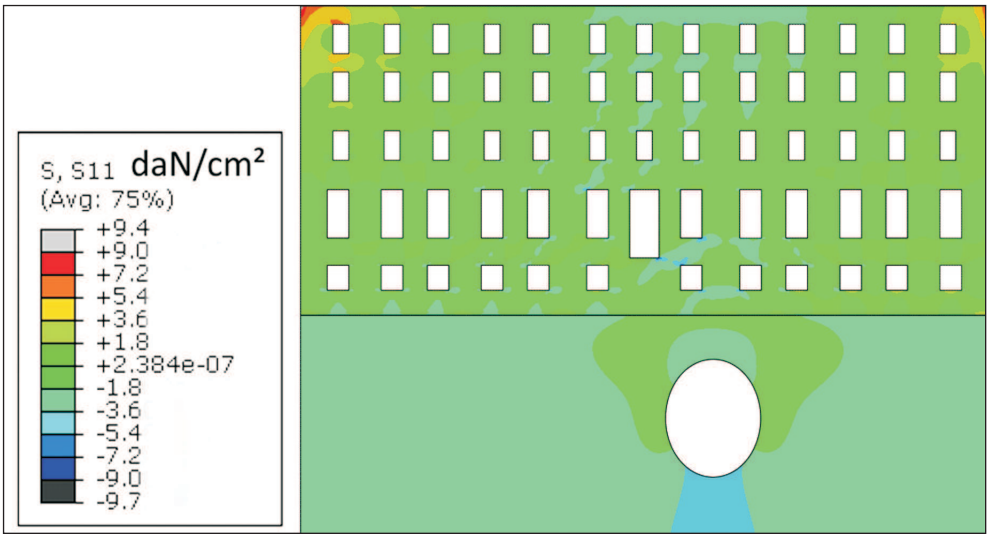

Figure 6. σ-stresses on vertical facets for scenario 3.

cavity located at 28.65 m from the left extremity of the wall are considered (Fig. 5):, (1) a 3.3 m wide cavity located between 3 m and 9.4 m in depth , (2) a 5 m wide cavity located between 7.8 m and 14.2 m in depth and (3) a 6.6 m wide cavity located between 3 m and 11 m in depth. After FE simulations, stress field maps are available (Fig. 6). As a support for the automatic interpretation, a single network of arbitrary density (Fig. 5) is proposed. Running the **[S]** module allows the extraction of results for every profile and then running the **[O]** module allows the computation of the virtually required reinforcements ($f_{steel,tension}$ = 500 MPa) at every profiles levels. The computed information is then graphically presented as rectangles corresponding to the reference grid (Fig. 7 left – no cavity) or disturbed grids (Fig. 7 centre – cavities in scenario 1, 2 or 3) depending on the analysed results file. In the coded grids, the profiles are adjacent to each other independently of their true geometrical position in the wall. Depending on the selected network, bays in the structural member may be guessed (dense and regular network) or not (loose and/or irregular network). The simultaneous observation of a disturbed grid and the reference one allows highlighting specific parasite tensions occurrences in some scenarios due to the presence of the cavity. Regarding the reasonable size of the considered wall and the fast analysis scheme implemented in the simplified post-processing tool, the computation time required to construct the grids remains limited. The deviation grids are computed using the **[C]** module (Fig. 7 right). These grids show the impact of the cavities on the north wall and provide the conventional reinforcement needed for each scenario to prevent damages. The application of the quantification **[Q]** module on the deviation grids gives NSI impact values of 93 (1), 180 (2) and 440 (3) respectively. These values show that the selected structural member is less sensitive to the presence of the cavity in scenario 1 than in scenario 2 and very less sensitive than in scenario 3.

5. Conclusions and perspectives

Due to the restrictions affecting the availability of lands, more and more building projects take place in zones characterized by the presence of karst features. The concomitant densification of surrounding activities increases the risks of stable ghost-rock karsts activation which might have a potential impact on vulnerable structures like URM buildings. Facing such situations, building specialists use FE simulations considering multi-scenarios approaches with coupled soil-structure models.

As the interpretation of FE results is time consuming, we proposed an automated approach to perform the post-processing of FE results. This approach is designed to be compatible with the daily engineering practices and the commercial modelling tools. In the proposed framework, the end-user performs in a first time his classical FE calculations, commonly opting for a large number of problematic scenarios. Then in a second time, the analysis network is defined within the interpretation tool. Through the setup of this network, the engineer focuses the interpretation scheme on key information. The process will act in any case but the sharper the stress field maps are discriminated, the higher the efficiency of the process will reveal. A good balance must be

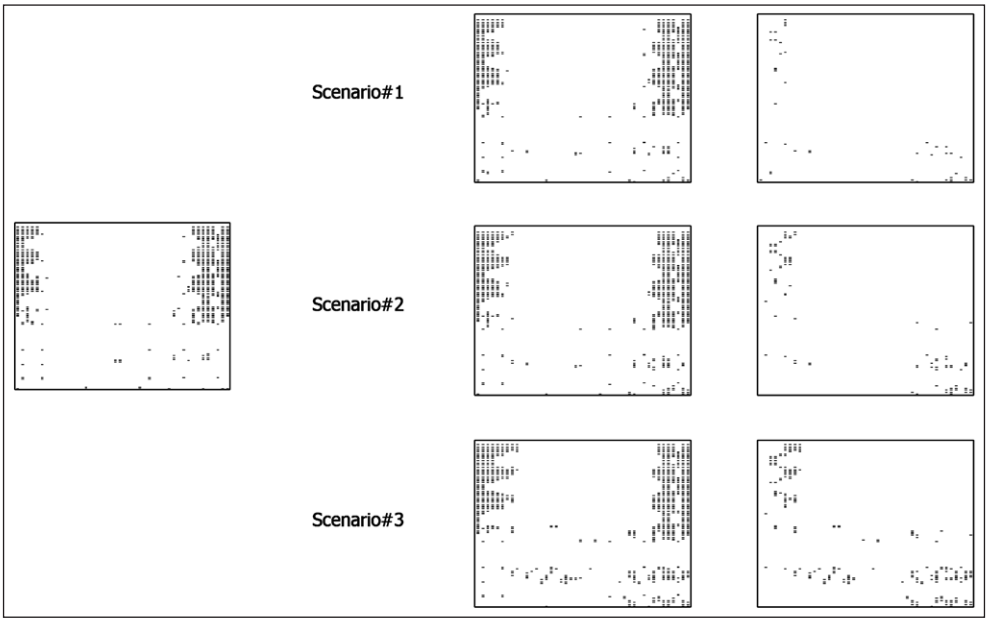

Figure 7. Reference grid (left), disturbed grids (centre), deviation grids (right).

found between the resolution of the analysis and the computing time required. The definition of the analysis network is therefore the most critical issue of the proposed methodology. It still remains a job for experts in building stability.

Following the definition of geological concepts to be integrated by building specialists implied in karst risk management, we described the articulation of the proposed methodology. We then illustrate our purpose by detailing the implementation of a simplified tool applied to a partial vulnerability study on an ancient URM building located in the Tournaisis.

The proposed methodology may prove efficient once implemented in an automatic interpretation tool. It offers the opportunity to quantify the impact of a given ground defect on a given structural member through a global indicator value. Using such network analysis opens the way to the establishment of objective functions in the field of optimization. Considering a morphological optimization approach, it is possible to search for the building patterns which are best fitted to critical zones regarding the geological nature of the karst risk. Through the achievement of further works, 'parakarstic guidelines', similar to the existing 'paraseismic guidelines' (e.g., Plumier & Doneux, 2003), might be edited. These guidelines would allow architects to integrate karst risk management since the early beginning of their work.

General optimization embedded in inverse problem solving should also be used *a posteriori* in order to outline the potential localization of the ground cavity based on the pathology pattern recorded on a damaged building. To improve the long-term management of karst risks in covered karst contexts, further works should focus on the combination of this method with permanent monitoring tools, such as geophysical methods, used to detect sinkholes migrating to the surface when ghost-rock features are activated.

6. Acknowledgements

We would like to thank M. Nicolas LAMANT for his practical contribution to the graphical content of the present paper. We also gratefully thank the invited Editor (C. Dubois) and two anonymous reviewers for their comments and suggestions. They were very much appreciated and helped improving the overall quality of the manuscript.

7. References

Buchignani, V., D'Amato Avanzi, G., Giannecchini, R. & Puccinelli, A., 2008. Evaporite karst and sinkholes: a synthesis on the case of Camaiore (Italy). Environmental Geology, 53, 1037-1044.

Buttrick, D.B. & van Schalkwyk, A., 1998. Cases and solutions: Hazard and risk assessment for sinkhole formation on dolomite land in South Africa. Environmental Geology, 36 (1), 170-178.

Deceuster, J., Delgranche, J. & Kaufmann, O., 2006. 2D cross-borehole resistivity tomographies below foundations as a tool to design proper remedial actions in covered karst, Journal of Applied Geophysics, 60 (1), 68-86.

Delvigne, J.E., 1998. Atlas of micromorphology of mineral alteration and weathering. The Canadian Mineralogist, Special Publication, ORSTOM Editions, France, 494 p.

Descamps, T., Van Parys, L., Noël, J. & Dagrain, F., 2011. Engineering and patrimonial buildings: rewarding interdisciplinary work. International Journal of Architectural Engineering, 5 (3), 315-333.

Domede, N., Pons, G., Sellier, A. & Fritih, Y., 2009. Mechanical behaviour of ancient masonry. Materials and structures / Matériaux et constructions, 42(1), 123-133.

Domede, N. & Sellier, A., 2012. Experimental and numerical analysis of behaviour of old brick masonries. Advanced materials research, 133-134, 307-312.

Dougherty, P., 2005. Sinkhole Destruction of Corporate Plaza Pennsylvania. Case study in: Waltham T., Bell F., Culshaw M., Sinkholes and subsidence – Karst and Cavernous Rocks in engineering and Construction. Proxis, Chichester U.K., 304-308.

Dubois, C., Quinif, Y., Baele, J.M., Dagrain, F., Deceuster, J. & Kaufmann, O., 2014. Mineralogical and petrophysical properties evolution of a weathered limestone in southern Belgium. Geologica Belgica, 17, 1-8.

Kaufmann, O., 2000. Les effondrements karstiques du Tournaisis : genèse, évolution, localisation, prévention. Speleochronos, Hors-Série, 350 p.

Kaufmann, O. & Deceuster, J., 2014. Detection and mapping of ghost-rock features in the Tournaisis area through geophysical methods – an overview. Geologica Belgica, 17 (1), 17-26.

Kaufmann, O., Deceuster, J. & Quinif, Y., 2012. An electrical resistivity imaging-based strategy to enable site-scale planning over covered palaeokarst features in the Tournaisis area (Belgium), Engineering Geology, 133-134, 49-65.

Kaufmann, O. & Quinif, Y., 1999. Cover-collapse sinkholes in the "Tournaisis" area, southern Belgium. Engineering Geology, 52, 15-22.

Kaufmann, O. & Quinif, Y., 2002. Geohazard map of cover-collapse sinkholes in the Tournaisis area, southern Belgium. Engineering Geology, 65, 117-124.

Kouroussis, G., Van Parys, L., Conti, C. & Verlinden, O., 2011. Prediction of environmental vibrations induced by railway traffic using a three-dimensional dynamic finite element analysis. Proceedings of the 13th international conference on civil, structural and environmental engineering computing, Chania (Greece).

Maunder, E., 1995. Thrust line solutions for masonry arches derived from finite element models. Arch bridges, Thomas Telford, London, 215-224.

Plumier, A. & Doneux, C., 2003. Guide technique parasismique belge pour maisons individuelles, SSTC, ULg, ORB, 121 p.

Quinif, Y., 2010. Fantômes de roche et fantômisation. Essai sur un nouveau paradigme en karstogenèse. Karstologia Mémoires, 18, 196 p.

Sowers, G.F., 1996. Building on sinkholes: design and construction of foundations in karst terrain. ASCE Press, 202 p.

Van Dijck, F. & Michel, R., 2006. Les risques naturels en Région Wallonne. Karst and Physical Planning International Colloquium, Namur, Belgium, 93-109.

Van Parys, L., Lamblin, D., Guerlement, G. & Descamps, T., 2006. Damage in patrimonial masonry structures: the case of the O-L cathedral in Tournai (Belgium). Solid Mechanics and its applications, 135, 209-216.

Vergari, A., Quinif, Y. & Charlet, J.M., 1995. Palaeokarstic features in the Belgian carboniferous limestones - implications to engineering. Karst geohazards: engineering and environmental problems in karst terrane. Proc. 5th conference, Gatlinburg 1995, 481-486.

Yuan, D., Li, B. & Liu, Z., 1998. Karst of China. In Yuan D., Liu Z. (eds). Global karst correlation. Science Press, Beijing, 167-177.

Manuscript received 15.12.2012, accepted in revised form 29.10.2013, available on line 15.11.2013